

Hubble Space Telescope imaging and ground-based spectroscopy of old nova shells – I. FH Ser, V533 Her, BT Mon, DK Lac, V476 Cyg

C.D. Gill¹ & T.J. O’Brien²

1. *Astrophysics Research Institute, Liverpool John Moores University, Twelve Quays House, Egerton Wharf, Birkenhead, L41 1LD*

2. *Jodrell Bank Observatory, The University of Manchester, Macclesfield, Cheshire, SK11 9DL*

30 November 2018

ABSTRACT

In this paper we report on the first five out of eleven observations in our programme of Hubble Space Telescope (HST) imaging of old nova shells. We present new WFPC2 images of the shells around FH Ser and V533 Her taken in the F656N (H α + [N II]) filter. We also show long-slit spectra taken using the William Herschel Telescope (WHT) in La Palma for these objects in the same spectral range.

The shell around FH Ser is found to be a prolate ellipsoid of ellipticity 1.3 ± 0.1 inclined at $62 \pm 4^\circ$ to the line of sight. The shell has an equatorial ring which is found to be due to increased emission in the two [N II] lines rather than H α . The expansion velocity is best modelled by a true equatorial expansion rate of 490 ± 20 km s⁻¹. The best-fitting systemic velocity is -45 km s⁻¹. A synthetic image and synthetic spectra are also presented for this model for comparison with our observations. We derive a distance to FH Ser of 950 ± 50 pc. The origin of the [N II] equatorial ring is discussed in the context of a photoionization feature resulting from aspherical illumination by the central source rather than a simple density enhancement. It is possible however that the ring is also in part due to an extremely localised increase in the nitrogen abundance. The brightest part of the shell was found to have a surface brightness of 9.1×10^{-15} erg cm⁻² s⁻¹ arcsec⁻².

Similar imaging and spectroscopy of the nova V533 Her reveal a shell of radius 5 ± 0.7 arcsec with an axial ratio of 1.2 ± 0.2 and peak surface brightness 1.3×10^{-15} erg cm⁻² s⁻¹ arcsec⁻². The expansion velocity of this shell is 850 ± 150 km s⁻¹ and the distance is estimated to be 1250 ± 300 pc.

The shells around BT Mon, DK Lac and V476 Cyg were not detected with HST implying 3σ upper limits to the surface brightness in H α + [N II] of 5.3 – 6.3×10^{-16} erg cm⁻² s⁻¹ arcsec⁻².

Key words: circumstellar matter – novae, cataclysmic variables

1 INTRODUCTION

Every classical nova outburst should result in the ejection of 10^{-5} to $10^{-4} M_\odot$ of material at velocities of the order of hundreds to thousands of kilometres per second (Bode & Evans 1989). Study of these expanding shells of nova ejecta has importance for a range of astrophysical areas including the physics of thermonuclear reactions, mixing mechanisms, nebular shaping, radiation-driven winds, clumping mechanisms, astrophysical chemistry and the formation of dust. Novae provide a real-time laboratory in which these processes can be investigated. The work presented in this series of papers builds on our ground-based imaging survey of the ejecta of old novae using 4-m class telescopes (Slavin, O’Brien & Dunlop 1995, Gill & O’Brien 1998) in two ways.

Firstly we present high-resolution imaging obtained with the Wide Field Planetary Camera 2 (WFPC2) on the Hubble Space Telescope (HST). This is then complemented by kinematical information obtained from spatially-resolved spectroscopy using the William Herschel and Anglo-Australian Telescopes (WHT & AAT respectively).

This first paper presents the HST images and medium-resolution long-slit WHT spectra of the shells of FH Ser and V533 Her in the region of H α . We also present non-detections in the HST imaging of BT Mon, DK Lac and V476 Cyg. §2 describes the observations and §3 presents the results. The data are interpreted and discussed in §4. The corresponding observations of HR Del, RR Pic, T Aur,

V1500 Cyg and V842 Cen will be presented in papers to follow.

2 OBSERVATIONS

Hubble Space Telescope (HST) observations of the novae were made during 1997/98 – see Table 1. In each case the nova was positioned on the Planetary Camera chip of WFPC2. The pixel scale is 46 mas with a complex point spread function distributing 60% of the flux from a point source over the 3×3 pixel region centred on the source.

The standard pipeline data processing was used (Leitherer 1995) and the images combined eliminating cosmic rays and bad pixels using standard tasks in STSDAS/IRAF. Narrow band photometry was performed using the prescription described by Dudziak and Walsh (1997). For the images where there was no immediately obvious detection of an ejected shell we applied a 7×7 sliding-box median-filter to the images to reduce the effects of noise and contamination from low level cosmic rays. This process enhanced the slower varying underlying background which is more consistent with an extended nova shell and thus allowed visual detection of shells to be investigated.

Long-slit spectra of the shells of FH Ser and V533 Her were taken on the 4.2m WHT in La Palma, Canary Islands using the ISIS spectrometer on 1996 Aug 3 – see Table 1. This instrument has the advantage of having both a blue and red arm which allows simultaneous observations of two wavelength ranges with a suitable dichroic. Using the TEK-1 and TEK-2 chips with the R1200B and R1200R gratings this instrument has a spectral range of 420\AA and a dispersion of $0.41\text{\AA}/\text{pixel}$ in both arms. Observations were taken with central wavelengths of $\lambda\lambda$ 4950 and 6600\AA for the blue and red arms respectively to allow primarily the lines of H α and H β ($\lambda\lambda$ 6562.8 and 4861.3\AA respectively) to be examined as well as [O III] ($\lambda\lambda$ 4959 and 5007\AA), [N II] ($\lambda\lambda$ 6549 and 6583\AA) and He I ($\lambda\lambda$ 4921, 5015 and 6677\AA). The dispersion along the slit was 0.36 arcsec per pixel. Slits of width 1 arcsec were used at position angles chosen to investigate features revealed in previous imaging. The spectra were reduced using standard techniques.

3 RESULTS

3.1 FH Ser

FH Ser (Nova Ser 1970) erupted in 1970 and was discovered by Honda (1970). It reached a peak visual magnitude of 4.4 on Feb 18 (Burkhead et al. 1970, Borra & Andersen 1970). The lightcurve shows a significant DQ-Her-type dip (e.g. Fig. 2 of Rosino et al. 1986) and is characterized by a t_3 time of 62 days (Duerbeck 1987). Recently it has been classified as a ‘slow’ nova belonging to the *Fe II* spectroscopic class (Della Valle & Livio 1998, Williams 1992). Duerbeck (1992) produced the first image of the shell from which he measured a radius of 2.7 arcsec and described an equatorial band of enhanced emission. He derived an orbital inclination of 58° and a distance of 850 pc. Later images were taken by Slavin et al. (1995) in 1993 September. Their images were deeper and in several narrow wavebands covering approximately $\lambda\lambda$ 6530 to 6608\AA . They also resolved the

equatorial enhancement and derived an inclination angle of $58 \pm 14^\circ$. They suggested that the equatorial band is due to H α emission from a density enhancement.

Della Valle et al. (1997) imaged this nova shell in 1996 March with a H α + [N II] filter. They showed the shell to be elliptical with outer diameters of 7.6 and 9 arcsec with a peak-to-peak minor axis of 5.4 arcsec. No peak-to-peak major axis was given. They also showed that the shell had an equatorial ring. They derived an inclination angle of 60° and a distance of 870 ± 90 pc.

3.1.1 Imaging

The FH Ser remnant was imaged with HST on 1997 May 11 with two 1200s integrations, Fig. 1. The maximum pixel value attributable to the shell is 10.9 counts (a $7\text{-}\sigma$ detection corresponding to a surface brightness of $9.1 \times 10^{-15} \text{ erg cm}^{-2} \text{ s}^{-1} \text{ arcsec}^{-2}$). The shell takes the form of a very clumpy limb-brightened prolate ellipsoid. There is a clear equatorial ring which is brighter in the western half compared to the eastern. If we assume this equatorial enhancement is an inclined circular ring then the derived inclination angle is $62 \pm 1^\circ$. The apparent major axis is 7.0 ± 0.3 arcsec and the minor axis 5.8 ± 0.1 arcsec (measured peak to peak). When this ellipsoid is de-projected the true axial ratio of the shell is found to be 1.26 ± 0.08 .

3.1.2 Spectroscopy

The long-slit spectra for both slit positions for the region of $6520\text{--}6610\text{\AA}$ are shown in Fig. 2. Both slits show velocity ellipses of the shell in the lines of H α (λ 6562.8 \AA) and [N II] (λ 6549 \AA and λ 6583 \AA). The only other detection of emission was from H β which has the same appearance as that of the H α ring. The two slit positions have been displayed using the same high and low levels to allow relative comparison of fluxes (it should be noted that the run was not photometric but a first order comparison is possible).

In slit position 1 the velocity ellipse in H α of the shell can clearly be seen between the two fainter [N II] ellipses. The H α ellipse shows clumpiness on small scales superimposed on a well defined velocity ellipse. The [N II] ellipses are both barely detected apart from a feature above (blue-shifted) and below (red-shifted) the central continuum source corresponding to the equatorial ring seen in the HST image. For the λ 6549 \AA line these features appear at $\lambda \sim 6538\text{\AA}$ and 6555\AA (within the H α ellipse), and for the λ 6583 \AA line they appear at $\lambda \sim 6573\text{\AA}$ (co-incident with the red-shifted H α ellipse) and 6591\AA . The fact that the equatorial ring feature above the stellar continuum (the west) is blue-shifted and the feature below is red-shifted indicates that the shell is inclined so that the western part of the shell is tilted away from the observer.

In slit position 2 the velocity ellipses are quite different to those in slit 1. The northern and southern halves look the same and the brightness of the [N II] λ 6583 \AA ellipse is comparable to that from the H α ellipse. The H α ellipse seems to be of fairly uniform intensity whereas the [N II] ellipse is brighter near the extremities of the shell (top and bottom of the slit). By inspection of the image in Fig. 1 it can be seen that the edges of the shell correspond with the

region where the equatorial ring is fully within the slit. The brightest region in the [N II] λ 6583Å ellipse is brighter than any region in the H α ellipse.

3.2 V533 Her

V533 Her (Nova Herculis 1963) was discovered by Dahlgren (1963) and extensively studied by Chincarini & Rosino (1964). It declined with a t_3 time of 44d (see Duerbeck 1981 using AAVSO light curves). However combining the V light curve presented by Chincarini (1964) which shows that it declined to 6th magnitude sometime between March 4 and 8 with the post-discovery results (see Haddock et al. 1963) that it actually reached magnitude 3 on Jan 30 shows it may be more accurate to quote a t_3 time of around 35d. It has been classified as a ‘slow’ nova belonging to the *Fe II* spectroscopic class (Della Valle & Livio 1997). The nebulosity around V533 Her was first detected by Cohen & Rosenthal (1983) by comparison with a point spread function. The first clear image was provided by Slavin et al. (1995) who detected a smooth circular shell, radius ~ 4.5 arcsec, with a thick equatorial band. This image is reproduced at the left of Figure 3.

3.2.1 Imaging

V533 Her was imaged with HST for a total of 2600s with 2 cosmic ray split observations on 1997 September 3. The median smoothed image of V533 Her is shown at the right of Figure 3. An approximately circular shell has been detected with radius ~ 5 arcsec, consistent with uniform expansion since the Slavin et al. epoch. The brightest knot at the bottom of the median-smoothed image of the shell has a maximum value of 1.8 counts per pixel corresponding to a 7σ detection at a surface brightness of 1.3×10^{-15} erg cm $^{-2}$ s $^{-1}$ arcsec $^{-2}$. The signal to noise in the HST image is however not sufficient to provide any more information than was already apparent from the earlier ground-based image.

3.2.2 Spectroscopy

WHT ISIS spectra were obtained on 1996 Aug 3. Two slit positions were used; slit 1 at PA 160° along the equatorial ring and slit 2 at PA 70° orthogonal to the equatorial ring. Both used a slit of width 1 arcsec. The two positions are indicated on the WHT image in Figure 3 reproduced from Slavin et al. (1995) but rotated to correspond to the orientation of the HST image shown alongside.

The spectra in the region of H α are shown in Figure 4 (the H β range is not reproduced here as, although the shell is just visible, the signal to noise is very poor). From these spectra we see that the radius of the shell at the first slit position is 4.5 ± 0.5 arcsec whilst at the second slit position this increases to 5.5 ± 0.5 arcsec. Hence there is some evidence that the shell is elliptical with an apparent axial ratio of 1.2 ± 0.2 . The major axis is orthogonal to the equatorial band which is consistent with a prolate ellipsoidal shell as observed in other novae e.g. FH Ser. We are unable to estimate an inclination and hence a true axial ratio as the equatorial band is not clearly detected in the HST

image. The maximum line of sight velocity (obtained from the points where the slits cross at the centre of the nebula) is estimated to be 850 ± 150 km s $^{-1}$. Expansion parallax, taking into account the estimated errors in the shell diameter and expansion velocity, leads to a distance estimate of 1250 ± 300 pc.

3.3 BT Mon

BT Mon reached maximum in 1939 September. The t_3 time is disputed in the literature due to the exact date of maximum light being missed. Payne-Gaposchkin (1964) quotes a t_3 of 36 days calculated from spectral data whereas Schaefer & Patterson (1983) quote a t_3 of 190 days from the light curve after maximum. The shell has been detected around this nova in spectroscopic observations by Marsh et al. (1983). The only image of the shell is that by Gill & O’Brien (1998). They claimed detection of a ring of emission of diameter ~ 7 arcsec after deconvolution of the image with various techniques.

BT Mon was imaged with HST in two observations for a total of 2500s. The median-smoothed image of BT Mon is shown in Fig. 5. No shell is detected putting a 3σ upper limit on the surface brightness of the shell at 6×10^{-16} erg cm $^{-2}$ s $^{-1}$ arcsec $^{-2}$.

3.4 V476 Cyg

V476 Cyg (Nova Cygni 1920) reached maximum on 1920 August 24. The measured t_3 time for its decline was 16.5d (Duerbeck 1987) classifying it as a very fast nova. A diffuse shell of radius ~ 5 arcsec was detected by Slavin et al. (1995). With their integration time of 900s it was barely detected above the 3 sigma level.

V476 Cyg was imaged with the HST for a total of 2600s (cosmic ray split by a factor 2). The median-smoothed image of V476 Cyg is shown at the top left of Fig. 5 where no nova shell is detected. This provides a 3σ upper limit to the shell surface brightness of 5×10^{-16} erg cm $^{-2}$ s $^{-1}$ arcsec $^{-2}$.

3.5 DK Lac

DK Lac (Nova Lacertae 1950) was discovered during its rise in 1950 January. The nova declined at a moderately fast rate with a t_3 of 32d, accompanied by large variations of brightness. Slavin et al. (1995) detected the shell around DK Lac, measuring its radius as 2.0 to 2.5 arcsec, although the shell is poorly distinguished from the central source.

The median-smoothed HST image of DK Lac (total integration time 2500s) is shown at the bottom left of Fig. 5. No shell is detected providing a 3σ upper limit on the shell surface brightness of 6×10^{-16} erg cm $^{-2}$ s $^{-1}$ arcsec $^{-2}$.

4 FURTHER INTERPRETATION OF THE FH SER RESULTS

4.1 Observations

The [N II] features seen in the spectrum from the first slit position (S1) directly above and below the central source and the [N II] features at the extremities of the shell in the

spectrum from the second slit position (S2) are associated with the equatorial ring clearly seen in the image. We would expect $H\alpha$ to mirror this behaviour if the ring results from an enhancement in density. However it can clearly be seen in S2 that $H\alpha$ is not greatly enhanced in the ring at all. The [N II] ring features in S1 are approximately 40 times greater than the typical [N II] flux in the rest of the shell; although the $H\alpha$ ellipse is rather clumpy in S1, there is no obvious comparative increase in brightness in the corresponding regions for the ring. Therefore the equatorial ring is dominated by enhanced emission in [N II].

This picture is supported by the images in Slavin et al. (1995). In their figure 3c they show an image of the FH Ser remnant taken with a filter central wavelength λ 6560Å, FWHM 17Å. From examining the long slit spectra shown in this paper we can see that this will include almost all light in $H\alpha$ apart from the parts of the shell moving directly towards or away from us. There should be no [N II] contamination. This image shows only a smooth ring of emission resembling a simple limb-brightened shell. There is no evidence in this image for an equatorial enhancement. Slavin et al. also show an image with filter central wavelength λ 6537Å, FWHM > 17Å (their figure 3a). From our spectra we can see that this corresponds primarily to blue-shifted [N II] λ 6549Å. This image shows a half-crescent of emission with very little emission in the rest of the shell which again implies the equatorial enhancement is an [N II] feature. This crescent of emission is to the west of the central source which agrees with our suggestion that the eastern pole is tilted towards us.

4.2 Synthetic Images and Spectra

Using the code described in Gill & O'Brien (1999) it is possible to produce synthetic images and spectra for simple models of the FH Ser nova shell. The code calculates emission as a function of density and therefore separate models needed to be produced for the $H\alpha$ and [N II] emission lines. The lines can be scaled relative to one another by arbitrary factors and then combined, taking into account the rest wavelengths of the lines and the Doppler shifting of each element, to produce a spectral cube for a given wavelength range.

To generate the synthetic spectra the spectral cube was then smoothed in the spatial directions with the equivalent of a 0.5 arcsec FWHM Gaussian to simulate the seeing of the ground-based observations. A 'slit' was then positioned on the cube at positions and widths to correspond with the observations. Smoothing must be performed before the slit is positioned onto the cube to allow light to be scattered into and out of the slit. The possibility of correction for a systemic velocity for any model was incorporated to allow a best fit to the data.

Synthetic images were generated by convolving the unsmoothed spectral cubes with the system throughput of the HST with the F656N filter (Leitherer 1995). This was approximated by a profile starting with zero throughput at λ 6545Å, rising linearly to peak at λ 6554Å, remaining constant to λ 6576Å, then falling linearly back to zero at λ 6582Å. The images were then generated by collapsing the filtered spectral cube in the spectral direction.

We have generated models corresponding to a thin prolate ellipsoidal shell with ellipticity 1.3 and inclination 62° .

For the [N II] components an equatorial enhancement by a factor of 40 in intensity was also added in a thin ring. The light from $H\alpha$ was increased by a factor of 8.6 relative to the typical (i.e. not the enhanced value appropriate to the ring) [N II] λ 6583Å line (to best fit the observations), and the [N II] λ 6549Å scaled by a factor 0.34 relative to the [N II] λ 6583Å line. Velocities were set proportional to the distance from the centre of the ellipsoid and the maximum line of sight velocity was set to be 530 km/s. For the model spectra to best fit the observations it was found that a systemic velocity of -45 km/s was required. The resulting synthetic spectra for positions S1 and S2 can be seen in Fig. 7 and the synthetic image in Fig. 6. The model agrees closely with the observations shown in Fig. 2. This also allows us to derive a distance to FH Ser of 950 ± 50 pc which takes full account of the asphericity of the shell.

If we examine the observed image in Fig. 1 we see that the equatorial ring is brighter in one half than the other, behaviour replicated in our synthetic image in Fig. 6. Our model shows that this is because the system throughput of the HST with the F656N filter lets through the red-shifted λ 6549Å light and the blue-shifted λ 6583Å light. Therefore the ring seen in the image isn't actually a whole ring from one line but two halves of the ring each from a different line. The ratio of the lines in this doublet is always $[6549]/[6583] = 0.34$, so the half of the ring visible in the image which is produced by the λ 6583Å line is 3 times brighter than the λ 6549Å half.

4.3 The origin of the [N II] ring

For the equatorial ring to be enhanced in [N II] relative to the rest of the shell requires either a density, ionization or metallicity effect.

A simple density increase would produce more [N II] (providing that the level did not start to become collisionally de-excited) but also more $H\alpha$ and is therefore presumably not the solution.

An increase in the amount of nitrogen in the equatorial plane of the FH Ser shell could explain the [N II] enhancement. There is the possibility of a metallicity variation across the surface of the white dwarf before eruption due to rotation of the white dwarf although it is difficult to see how a thin enhancement of nitrogen could be produced rather than a more wide-spread variation around the shell.

The final possibility is an ionization effect which would require either an increase or decrease in ionization in the equatorial region. A good candidate for providing such an effect is the accretion disc around the central source. An explanation could be that the main shell is very highly ionized, doubly ionized or above, by the central parts of the accretion disk. The equatorial region is then shadowed from this hot central UV source, causing the relative abundance of nitrogen in the singly ionized state to be increased. This would then produce an increase in [N II] emission in a thin equatorial region with no increase in $H\alpha$. This proposal needs testing by further observation and modelling. A similar suggestion was made by Petitjean et al. (1990) for the shell of DQ Her.

5 CONCLUSIONS

HST WFPC2 images and WHT spectroscopy of FH Ser have allowed us to derive a consistent model for its shell as an ellipsoid with ellipticity 1.3 ± 0.1 , and inclination $62 \pm 4^\circ$. The equatorial expansion rate is found to be $490 \pm 20 \text{ km s}^{-1}$ and the systemic velocity -45 km s^{-1} . This gives a distance to FH Ser of $950 \pm 50 \text{ pc}$. These values agree within the errors with the results presented in previous papers (Della Valle et al. 1997, Slavin et al. 1995, Duerbeck 1992). The equatorial ring seen in the HST images and previous ground-based images is found to be due to a $40\times$ increase in emission from [N II] rather than $\text{H}\alpha + [\text{N II}]$. It is suggested that the origin of this ring lies either in abundance gradients in the shell or in aspherical illumination of the shell by the central photoionizing source. This latter suggestion will be developed in a paper to follow.

Similar imaging and spectroscopy of the nova V533 Her reveal a shell of radius $\sim 5 \text{ arcsec}$ with an axial ratio of 1.2 ± 0.2 . The expansion velocity of this shell is $850 \pm 150 \text{ km s}^{-1}$ and the distance is estimated to be $1250 \pm 300 \text{ pc}$. The quality of the data is however not sufficient for us to examine the structure of the shell in as much detail as was possible for the shell of FH Ser.

Our HST images of BT Mon, V476 Cyg and DK Lac provided only upper limits on the surface brightness of their shells. This may seem surprising given that these shells had been previously detected from the ground (Gill & O’Brien 1998, Slavin et al. 1995). However it should be noted that the ground-based images were taken using the large aperture 4.2m WHT and 3.9m Anglo-Australian Telescope. Although the improved spatial resolution of HST helps overcome its reduced collecting area when the nebula is clumpy and these clumps are unresolved from the ground this does not apply when the emission is more smoothly distributed. These nova shells were not particularly well-detected in the ground-based survey (BT Mon requiring image deconvolution) so it is perhaps not too surprising that we did not detect them here.

Other novae to be investigated in the following papers of this series include HR Del, RR Pic, T Aur, V842 Cen and V1500 Cyg.

6 ACKNOWLEDGEMENTS

We would like to thank Dr M. Della Valle for valuable comments at the refereeing stage. CDG would like to thank PPARC for his studentship, and Nial Tanvir and Rachel Johnson for their help with the reduction of the HST images. This work is based on observations with the NASA/ESA Hubble Space Telescope (obtained at the Space Telescope Science Institute, which is operated by the Association of Universities for Research in Astronomy, Inc. under NASA contract No. NAS5-26555) and the William Herschel Telescope (operated on the island of La Palma by the Isaac Newton Group in the Spanish Observatorio del Roque de Los Muchachos of the Instituto de Astrofísica de Canarias).

REFERENCES

- Bode M. F., Evans A., 1989, *Classical Novae*, Wiley & Sons Ltd., Chichester
- Borra E.F., Andersen P.H., 1970, *PASP*, 82, 1070
- Burkhead M.S., Seeds M.A., Lee V.J., 1970, *IAU Circ* 2220
- Chincarini G., Rosino L., 1964, *Ann. d’Astrophys.*, 27, 469
- Chincarini G., 1964, *PASP*, 76, 289
- Dahlgren E., 1963, *IAU Circ* 1817
- Della Valle M., Gilmozzi R., Bianchini A., Esenoglu H., 1997, *A&A*, 325, 1151
- Della Valle M., Livio M., 1998, *ApJ*, 506, 81
- Dudziak G., Walsh J.R., 1997, *HST Calibration Workshop*, Baltimore, STScI, eds. Casertano S. et al.
- Duerbeck H.W., 1981, *PASP*, 93, 165
- Duerbeck H.W., 1987, *A Reference Catalogue and Atlas of Galactic Novae*, D. Reidel Publishing Company, Dordrecht & Boston
- Duerbeck H.W., 1992, *AcA*, 42, 85
- Gill C.D., O’Brien T.J., 1998, *MNRAS*, 300, 221
- Gill C.D., O’Brien T.J., 1999, *MNRAS*, 307, 677
- Haddock F.T., Howard W.E., Malville J.M., Seling T.V., 1963, *PASP*, 75, 456
- Honda, 1970, *IAU Circ* 2214
- Kohoutek L., 1981, *MNRAS*, 196, 87P
- Leitherer C., 1995, *HST Data Handbook Version 2*, Baltimore, STScI
- Petitjean P., Boisson C., Pequignot D., 1990, *A&A*, 240, 433
- Rosino L., Ciatti F., Della Valle M., 1986, *A&A*, 158, 34
- Slavin A.J., O’Brien T.J., Dunlop J.S., 1995, *MNRAS*, 276, 353
- Williams R.E., 1992, *AJ*, 104, 725

HST WFPC2 Imaging				
Nova	Epoch	Filter	Integration time	
FH Ser	1997 May 11	F656N	2×1200s	
V533 Her	1997 Sep 3	F656N	2×1300s	
BT Mon	1997 Apr 26	F656N	2× 1200s	
DK Lac	1998 Mar 28	F656N	2×800s + 1×900s	
V476 Cyg	1997 Aug 5	F656N	2×1300s	

WHT ISIS Spectroscopy					
Nova	Epoch	Wavelength range	Grating	Integration time	Slit PA
FH Ser	1996 Aug 3	4740–5160Å	1200B	2×900s	84° 174°
		6390–6810Å	1200R	2×900s	84° 174°
					160° 70°
V533 Her	1996 Aug 3	4740–5160Å	1200B	2×1800s	160° 70°
		6390–6810Å	1200R	2×1800s	160° 70°

Table 1. Details of the HST WFPC2 imaging and WHT ISIS spectroscopy presented in this paper. The F656N filter has central wavelength 6560 Å and full width at half maximum of 30 Å. Slit widths were 1 arcsecond.

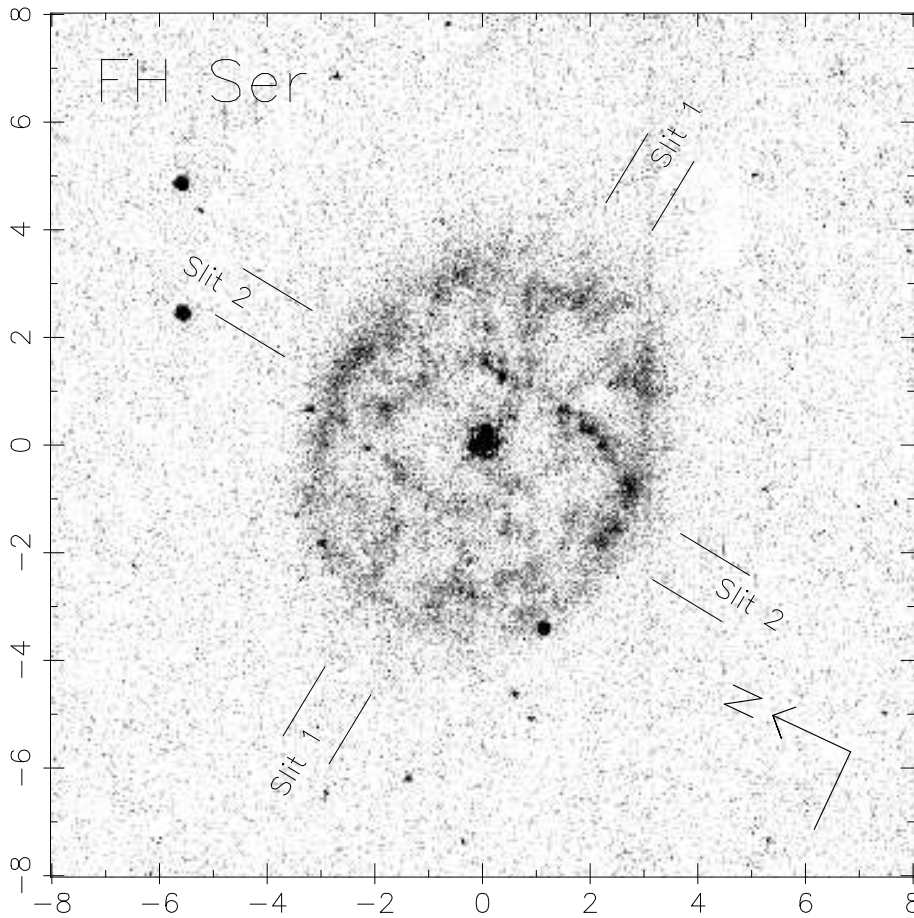


Figure 1. HST F656N image of the remnant around FH Ser. The orientation of the image is shown with the arrow towards north and the plain line to east. The slit positions for spectroscopy are shown with 1 arcsec slits.

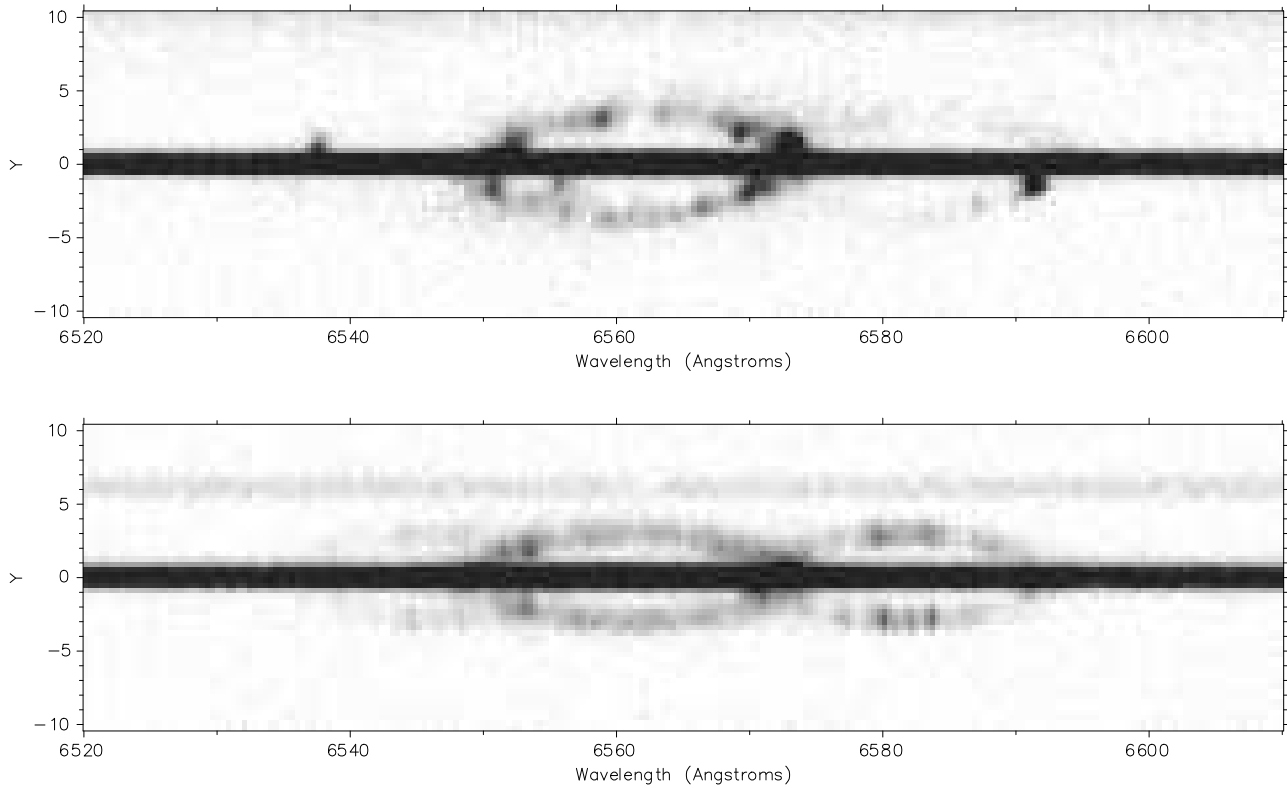


Figure 2. Long slit spectra for the shell of FH Ser in slit positions 1 (top) and 2 (bottom). In slit 1 west is to the top of the frame and in slit 2 north is to the top. The spatial direction is labelled as Y in both slits and is marked in arcseconds.

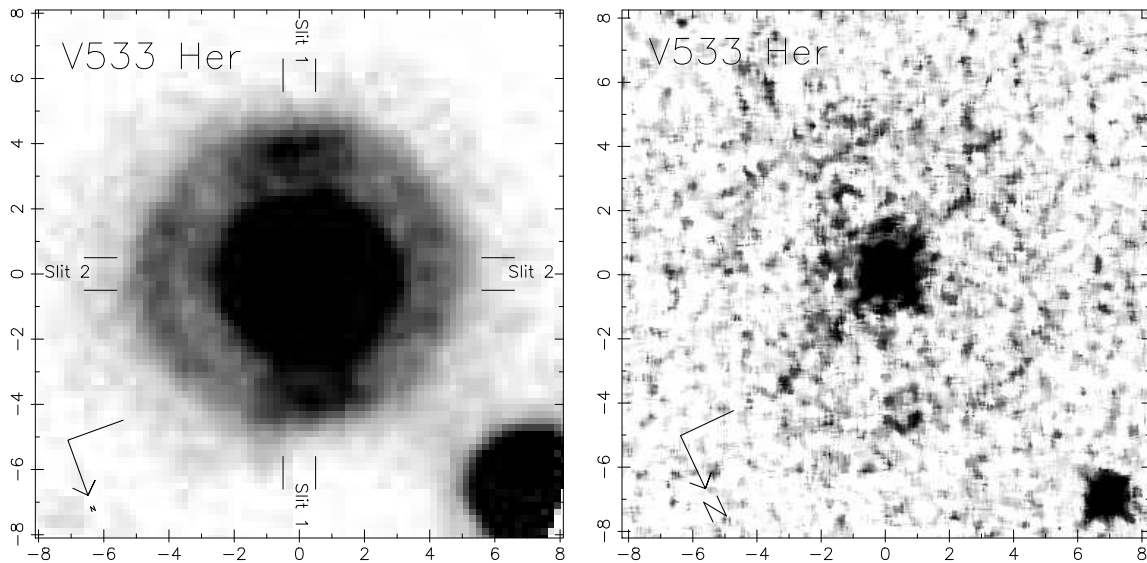


Figure 3. Ground-based image showing the positions of slits for the spectroscopy of the V533 Her shell (left) shown next to HST F656N image of the V533 Her shell (right). The ground-based image shown is a $H\alpha$ narrow-band image taken from Slavin et al. (1995). The HST image has been processed with a 7×7 sliding-box median-filter and is shown scaled between the background and 5σ above the background. All axes are marked in arcseconds from the central source.

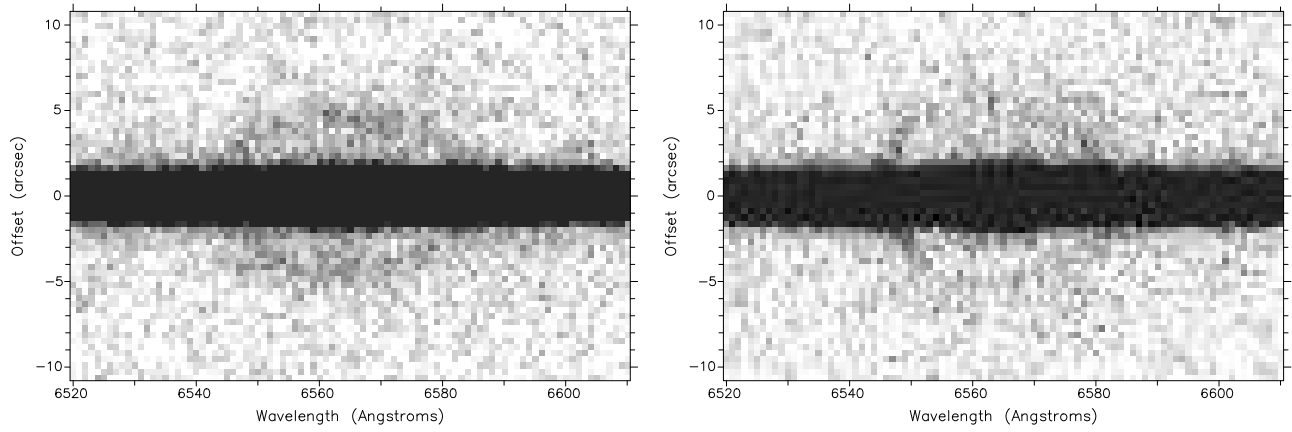


Figure 4. Long slit spectra of the shell around V533 Her. Slit 1 (left) is positioned across the equatorial ring whereas Slit 2 (right) is perpendicular to the equatorial ring. These spectra have been binned to $1\text{\AA}/\text{pixel}$ to make the velocity ellipses more apparent.

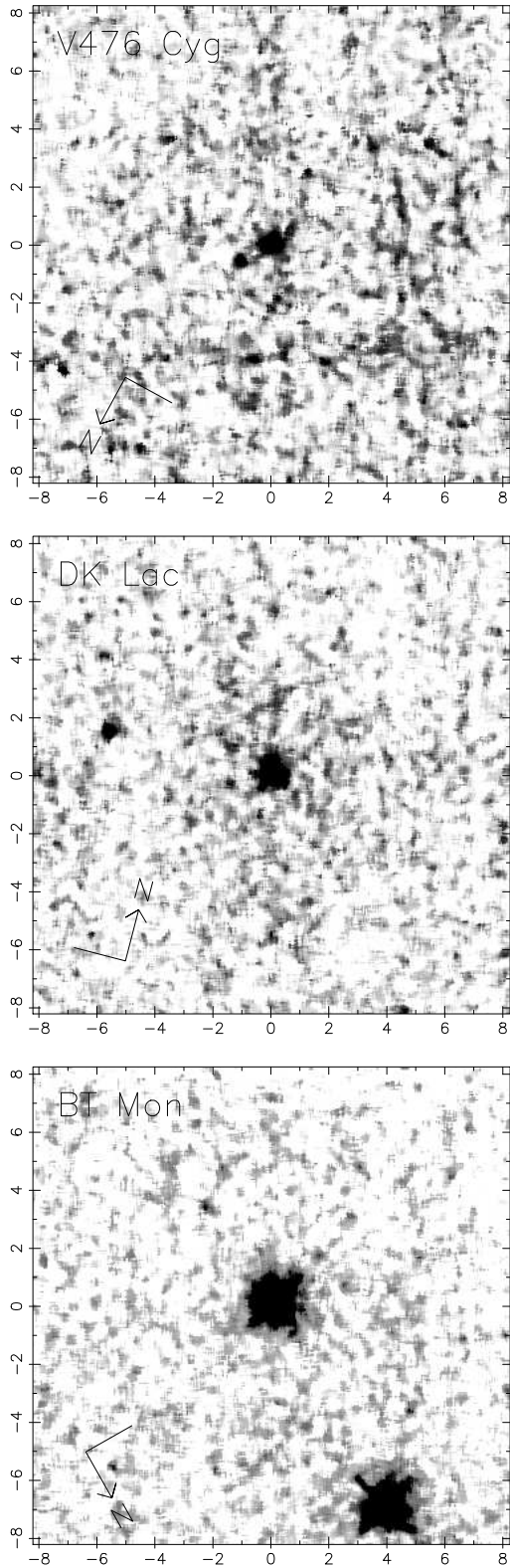


Figure 5. 7×7 sliding-box median-filtered F656N ($H\alpha + [N II]$) images for V476 Cyg (top), DK Lac (middle) and BT Mon (bottom). All images are scaled between the background level and 5σ of the background above the background level. All axes are marked in arcseconds from the central source.

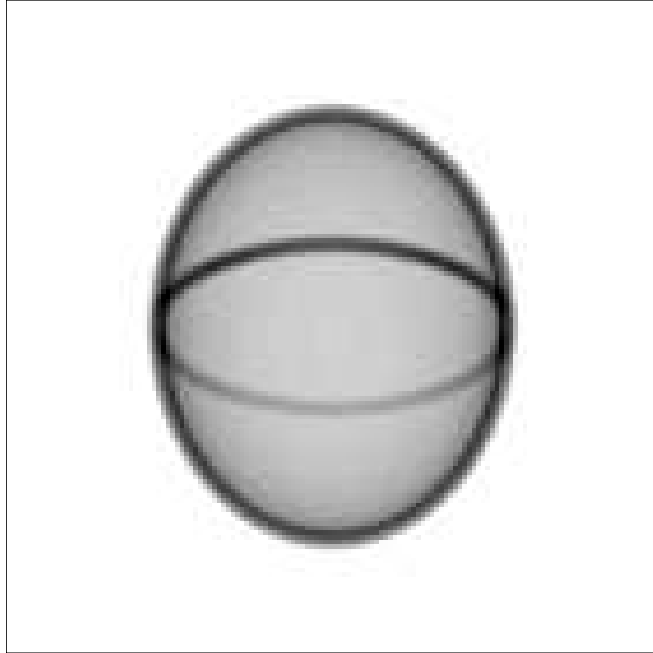


Figure 6. Simulated HST F656N image of the remnant around FH Ser containing contributions from $H\alpha$ and $[N II]$.

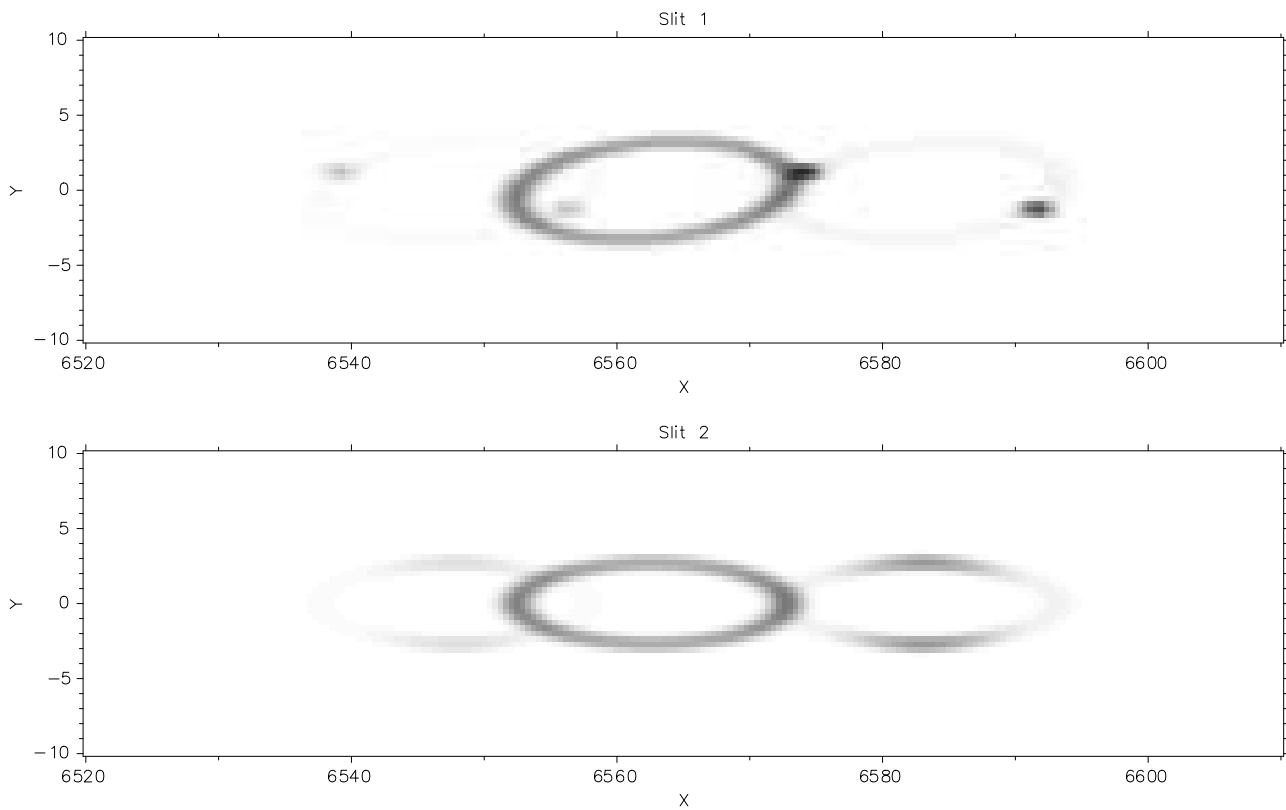


Figure 7. Synthetic long slit spectra for the shell of FH Ser in slit positions 1 (top) and 2 (bottom). In slit 1 west is to the top of the frame and in slit 2 north is to the top. The spatial direction is labelled as Y in both slits and is marked in arcseconds. The spectral direction, labelled X , is marked in Angstroms.